

Integrated CO₂ Capture and Mineralization Based on Monoethanolamine and Lime Kiln Dust

Liang Li,* Hai Yu,* Graeme Puxty, Song Zhou, William Conway, and Paul Feron



Cite This: *Ind. Eng. Chem. Res.* 2024, 63, 16019–16028



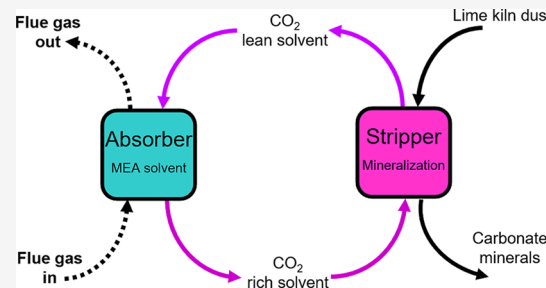
Read Online

ACCESS |

Metrics & More

Article Recommendations

ABSTRACT: Development and deployment of innovative and cost-effective CO₂ capture and utilization technologies can not only reduce the amount of CO₂ currently in or being emitted into the atmosphere but also develop a circular economy and deliver economic growth. Differing from previous studies on amine-based CO₂ capture in isolation, the work herein is focused on an integrated CO₂ capture and mineralization approach with monoethanolamine (MEA) as CO₂ liquid absorbent and utilization of lime kiln dust (LKD) as the CO₂ mineralization feedstock to regenerate or recover MEA used for CO₂ capture. Aqueous solutions containing 2.0 M MEA were used to capture CO₂ from a simulated flue gas comprising a CO₂ concentration of 10.0% (by volume) prior to the addition of LKD powders to precipitate captured CO₂ in the MEA solution through carbonation reactions. Following CO₂ mineralization, MEA filtrate was collected and analyzed by FTIR and ICP-OES, with solid materials undergoing chemical analysis by TGA and SEM, and additionally for particle size. The CO₂ mineralization process was found to be significantly influenced by the solution pH and temperature of the MEA absorbent solution, where conditions below pH 10.5 restrained CO₂ mineralization due to the limited availability of carbonate ions. Conversely, under higher pH conditions, the conversion of carbamate and bicarbonate to carbonate is promoted, accelerating the CO₂ mineralization process. Increasing the absorbent temperature (i.e., from 40.0 to 60.0 °C) resulted in a corresponding and considerable increase in the CO₂ mineralization rate and the CO₂ desorption efficiency of MEA. Following mineralization, the CO₂ desorption efficiency of CO₂-loaded MEA reaches 79–83%. The CO₂ sequestration capacity of LKD was determined to be ~230 g CO₂ per kg, with calcite and aragonite forms as the major calcium carbonate products formed during the CO₂ mineralization processes.



1. INTRODUCTION

Carbon capture, utilization, and storage (CCUS) is playing a critical role in reducing hard-to-abate CO₂ emissions of heavy industries.^{1–3} Currently, postcombustion carbon capture (PCC) has been one of the most developed techniques considered for CO₂ capture from flue gases emitted by industries. Existing PCC technologies are based mainly on liquid absorbents, membranes, solid adsorbents, electrochemical separation, etc.^{4–8} PCC using aqueous amine solutions is among the leading technology for large-scale industrial CO₂ capture.^{4,5} As of 2022, more than 20 amine-based carbon capture projects are at different stages of development.⁹ The typical CO₂ capture process based on the amine scrubbing method is shown in Figure 1, where flue gas containing CO₂ following combustion is contacted with an aqueous amine solution in an absorber column in which CO₂ absorption takes place. Following absorption, the CO₂-lean flue gas is washed and released into the atmosphere. CO₂-loaded amine solutions are then transferred to a stripping process where the temperature is increased to ~120 °C and/or the pressure is reduced to release the absorbed CO₂ and to recover the amine solutions.^{10–12} CO₂-lean amine solution is

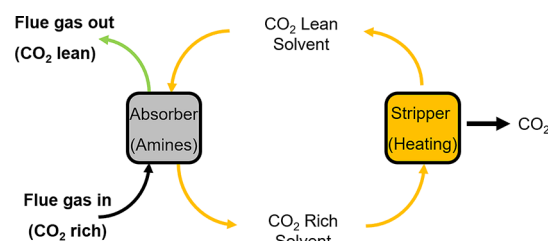


Figure 1. Schematic of a typical PCC process utilizing amine-based absorbents.

subsequently cooled and reused in the absorber for CO₂ capture, making the carbon capture process cyclical.

Received: June 1, 2024

Revised: August 21, 2024

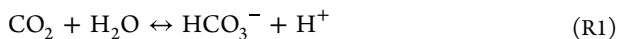
Accepted: August 22, 2024

Published: August 29, 2024

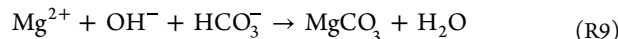
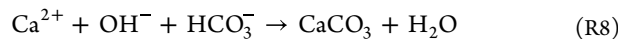


In the assessment of the suitability of amine-based CO₂ capture technologies for industrial applications, a wide range of factors must be considered, including but not limited to the technological features and the availability and cost of utilities. The widespread deployment of carbon capture technologies still faces many technical challenges, specifically the considerable energy consumption required for the recovery and regeneration of amines through heating and degradation of the amine absorbents under industrial capture conditions.^{5,13–16} In an attempt to address these two barriers, this study further investigates a novel CO₂ mineralization method as an alternative approach to the absorbent regeneration process, specifically the reduction of the elevated heating requirement for amine solutions. Importantly, the incorporation of CO₂ mineralization into amine-based carbon capture technologies can not only potentially reduce the consumption of electricity and heat duties but also achieve permanent CO₂ sequestration and production of products, thereby reducing the costs and risks for CO₂ storage and transportation.

Generally, the CO₂ absorption liquids are based mainly on aqueous solutions of an amine (e.g., monoethanolamine (MEA) or diethanolamine).^{5,10,12,17} Blended alkanolamines and ammonia are also used to increase the absorption rate, lower the solvent regeneration energy, or increase the oxidative resistance.⁵ The literature^{18–20} on amine solutions is abundant with mechanistic insights into the CO₂ absorption chemistry for the commonly used absorbents, which are considered well-understood at this stage in their maturity. The primary CO₂ absorption reactions in monoamines can be described by reactions R1–R7.



The absorbed CO₂ in the amine solutions primarily exists in the forms of carbamate from the direct reaction with primary and secondary amines, and bicarbonate from the decomposition of carbamate as a result of steric hindrance or at relevant pH conditions, as well as from the reaction of CO₂ with small amounts of hydroxide formed in the solutions. It is postulated that after incorporation of calcium and magnesium minerals into the CO₂-loaded amines for CO₂ mineralization, bicarbonate ions can be converted into calcium/magnesium carbonate precipitation as shown in reactions R8 and R9, thereby restoring the amine solutions for further absorption cycles.^{21–25} A wide range of alkaline solid materials as CO₂ mineralization feedstocks have been investigated in recent years, including concrete wastes, blast furnace slags, fly ash, cement kiln dust, and ultramafic mine tailings among others.^{26,27} Generally, elevated content of calcium and magnesium phases suitable for CO₂ mineralization (e.g., calcium/magnesium oxide and calcium/magnesium silicates) promotes higher CO₂ sequestration capacities.



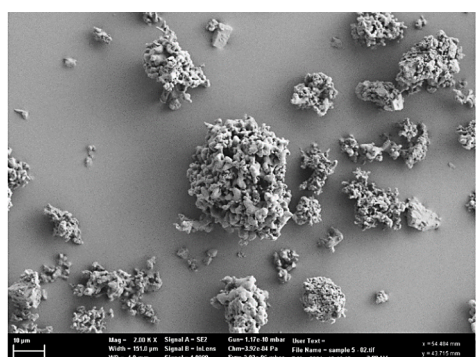
In an effort to explore the chemical effects of CO₂ mineralization on the regeneration of amine-based CO₂ absorption liquids, the integrated CO₂ capture and mineralization based on MEA and lime kiln dust (LKD) was investigated here. Broadly speaking, the focus of this work includes (i) the investigation of chemical phenomena and demonstration of the general chemical processes of an integrated CO₂ capture and mineralization process using aqueous MEA as a base case; (ii) exploring avenues for optimization and tuning of conditions for rapid and efficient CO₂ desorption of an aqueous MEA solution utilizing CO₂ mineralization; (iii) elaborate on the specific chemical mechanisms underpinning the regeneration of MEA by CO₂ mineralization; and (iv) characterization of the carbonation features of LKD powders for CO₂ mineralization applications. Encompassing existing and acquired knowledge in this work, discussion of the ongoing research gaps and prospects for the development of integrated CO₂ capture and mineralization technologies are also identified and analyzed in-depth.

2. EXPERIMENTAL STUDY

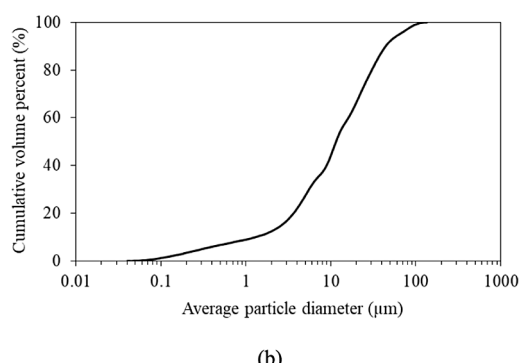
2.1. Liquid and Solid Used for CO₂ Capture and Mineralization.

MEA (assay $\geq 99\%$) was purchased from Sigma-Aldrich. High-concentration MEA solutions between 15% and 30%^{4,5,28,29} (approximately equal to 2.0–5.0 mol/L) are typically employed for industrial CO₂ capture, while from the viewpoint of CO₂ mineralization, a lower MEA concentration (from 0.1 to 2.0 mol/L)^{22–25} is seen as more desirable. Considering the combined capture and mineralization processes here, a 2.0 mol/L MEA solution was selected. The LKD raw material, as a byproduct during the manufacturing of quicklime (calcium oxide) from limestone in a lime kiln, was collected from a local lime plant in Australia. Primary oxide compositions of the LKD measured by X-ray fluorescence include (wt %): CaO (78.3%), SiO₂ (1.1%), MgO (0.9%), and loss of ignition (18.3%). Scanning electron microscopy (SEM) was performed on the LKD samples using the Zeiss Sigma VP field-emission SEM, while particle size distribution was measured by a Saturn DigiSizer II 5205 laser diffractometer. An example SEM image of LKD samples is shown in Figure 2a, and the particle size distribution is shown in Figure 2b. The average particle size (D₅₀) determined for the LKD here is approximately 15 μm .

2.2. Experimental Studies. 2.2.1. *CO₂ Capture.* A gas mixture containing CO₂ and nitrogen with a CO₂ concentration of 10.0% was used to simulate a typical postcombustion carbon capture flue gas. The experimental setup for the CO₂ capture measurements using 2.0 M MEA solutions is shown in Figure 3. A Drechsel gas washing bottle (QUICKFIT) fitted with fritted distribution heads (zero porosity) was used to sparge the gas mixture into the MEA solutions. To minimize moisture loss from the MEA solution during CO₂ loading, the 10.0% CO₂ gas was initially humified by passing the inlet gas through ultrapure water in a presaturator. A chilling condenser was additionally employed to reduce any loss of MEA. The gas flow rate was controlled by Sever Star mass flowmeters with a set point of 90.0 L/h. The CO₂ concentration of the inlet and outlet gas was monitored using a Horiba VIA 510-ES 510 CO₂ gas analyzer. The pH of the MEA solution was monitored



(a)



(b)

Figure 2. (a) SEM image of LKD used as a CO₂ mineralization feedstock and (b) particle size distribution curve.

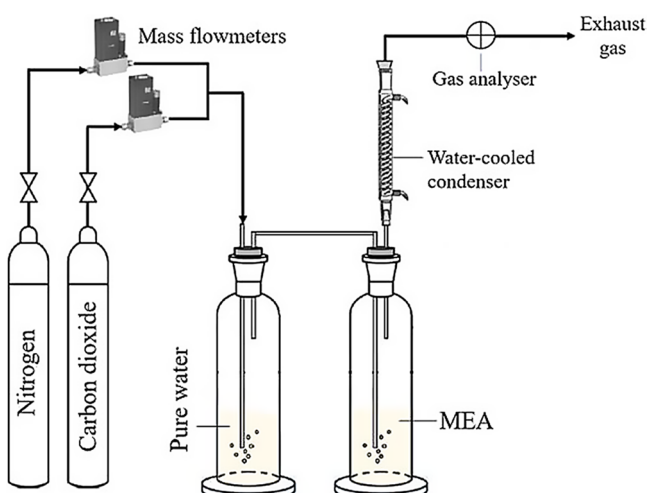


Figure 3. Experimental setup for CO₂ absorption using 2.0 M MEA solution.

throughout by an Orion Star A211 Benchtop pH meter. The CO₂ concentration in the MEA solution was determined by Fourier-transform infrared spectroscopy (FTIR) analysis using ALPHA II compact FTIR spectrometer through a principal component regression based on an independent calibration method that has been described in detail previously.³⁰ In the literature,^{28,29,31} similar utilization of FTIR for CO₂ absorption of MEA solutions are also reported.

2.2.2. CO₂ Mineralization. After the MEA solutions were loaded with CO₂, mineralization was initiated to decarbonize the CO₂-loaded MEA solution, recovering and restoring its CO₂ capture capacity. The experimental setup for the CO₂

mineralization of an aqueous MEA solution utilizing LKD is shown in Figure 4. Broadly, an amount of LKD solid was

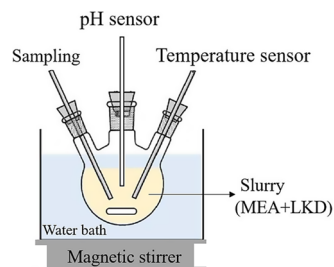


Figure 4. CO₂ mineralization and regeneration apparatus for a 2.0 M MEA solution.

initially added into the CO₂-loaded MEA at a specific solid-to-liquid ratio to form a slurry. The LKD slurry was further subjected to magnetic stirring (speed setting at 800 rpm) to homogenize the mixture. The solution pH and temperature of the slurry were monitored to follow the progress of the mineralization process. Liquid samples were continuously extracted with the separation of solid and liquid components undertaken using 0.45 μm membrane filters. Thermogravimetric analysis (TGA) of the filter cake (i.e., mineralized or carbonated LKD residue) was performed. Elemental concentration (in particular, calcium) in the MEA filtrate was determined using an Agilent 5900 inductively coupled plasma optical emission spectroscopy (ICP-OES) instrument. Prior to analysis, MEA filtrate was diluted and acidified to a 5.0% HNO₃ solution. The reaction temperature was controlled throughout using a circulating water bath, allowing for the determination of the temperature dependence of the mineralization reactions.

2.3. Characterization and Data Analysis of Liquid and Solid. The TGA/DSC 1 instrument manufactured by Mettler-Toledo (Switzerland) was used to carry out the thermodynamic analysis of LKD before and after CO₂ mineralization. Following TGA analysis, the sequestered CO₂ by mineralization of LKD was determined by eq 1.

$$\Delta M_{\text{CO}_2} = \frac{\Delta M_{\text{TGA},1}}{M_1} - \frac{\Delta M_{\text{TGA},2}}{M_2} \quad (1)$$

where M₂ and M₁ are the masses of LKD samples pre- and post-CO₂ mineralization after dewatering at 105.0 °C. ΔM_{TGA,1} and ΔM_{TGA,2} are the mass loss of LKD samples with and without CO₂ mineralization between 550 and 780 °C (i.e., temperature interval of decomposition of calcium carbonate), respectively.

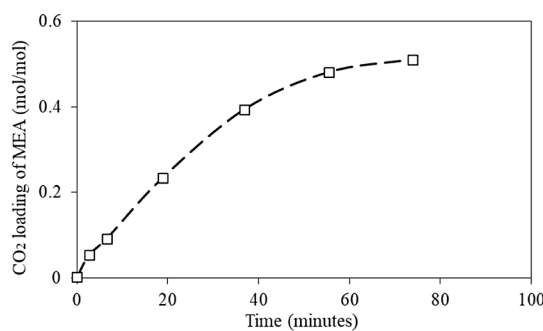
From the FTIR analysis of the MEA liquids following mineralization, the CO₂ desorption efficiency was calculated by eq 2.²²

$$\varnothing = \frac{\gamma_0 - \gamma_c}{\gamma_0} \times 100\% \quad (2)$$

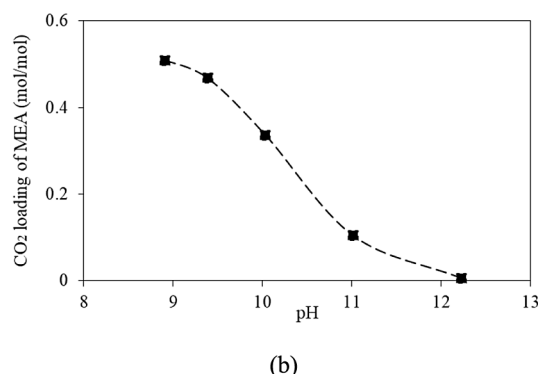
where γ₀ and γ_c are the CO₂ loadings of MEA pre- and post-CO₂ mineralization, respectively.

3. RESULTS AND DISCUSSION

3.1. CO₂ Capture of MEA from Flue Gas. The measured CO₂ absorption of 2.0 M MEA from the simulated flue gas is shown in Figure 5a. After ~60 min of sparging (~90.0 L/h/g gas



(a)



(b)

Figure 5. CO₂ capture process of 2.0 M MEA (a) CO₂ loading of MEA by 10% CO₂ gas and (b) variation of CO₂ loading over pH of MEA solvent.

flow rate and 10% v/v CO₂ concentration), the CO₂ loading gradually stabilizes, reaching equilibrium with the gas at around 0.51 mol/mol. Additional sparging was performed to ensure complete equilibrium was established (75 min CO₂ loading time total), at which point the pH of the 2.0 M MEA solution was measured (approximately pH = 9), and the CO₂ loading process was halted. The measured pH of the 2.0 M MEA solution as a function of the measured CO₂ loading is shown in Figure 5b. Prior to the initiation of the CO₂ loading process, the pH of the 2.0 M MEA solution was initially \sim 12.2, which subsequently reduced during the CO₂ absorption process until equilibrium around pH = 9 at CO₂ saturation (room temperature and pressure). Due to the chemistry of the MEA solutions and dynamic changes in the chemical composition, as CO₂ is additionally absorbed, the pH change of the solutions is nonlinear throughout. Notably, as the pH of the MEA solution is reduced from 11 to 9.4, the apparent change in the CO₂ loading of the solution increases significantly. According to ¹³C NMR results previously reported by Lv et al. (2015),¹⁹ when the pH of the CO₂-loaded MEA solution was higher than \sim 9.0, the amount of HCO₃⁻/CO₃²⁻ in the solution is negligible, while the ratio of carbamate and protonated MEA is prevailing. To guide our understanding of the effect of solution composition on the underlying mineralization phenomena, the concentrations of bicarbonate(HCO₃⁻)/carbonate(CO₃²⁻)/carbamate-(AmCOO⁻) species in the CO₂ loaded MEA were calculated using a reported thermodynamic model for the CO₂-H₂O-amine system.^{20,32} The resulting concentration profiles are presented in Figure 6. From the calculations, the bicarbonate concentration in the solution could be expected to be lower than 0.1 M at the equilibrium CO₂ loading approaching 0.50–

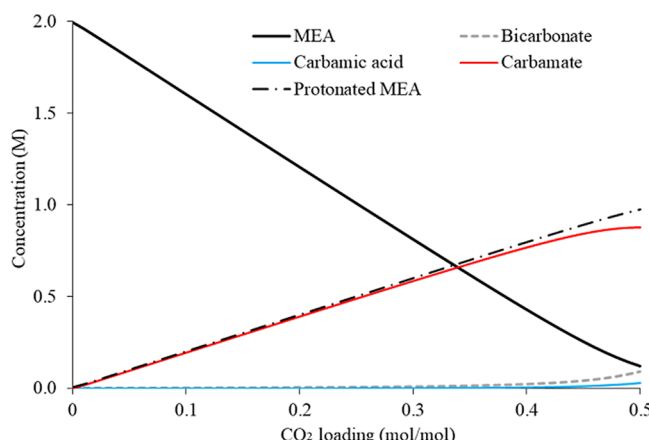


Figure 6. Concentration profiles of the MEA/MEA⁺ and carbon species in the 2.0 M MEA solution as a function of the CO₂ loading.

0.55 mol/mol. Theoretically, such a low bicarbonate concentration is seemingly nonfavorable for direct CO₂ mineralization (see reactions R8 and R9). Therefore, the decarbonation or the regeneration of MEA through CO₂ mineralization is expected to proceed via the decomposition of carbamate to bicarbonate.

3.2. Recovery of CO₂-Loaded MEA by Mineralization.

3.2.1. Multistep CO₂ Mineralization Method. After the CO₂ loading process, a multistep CO₂ mineralization approach was initially undertaken at ambient temperature to regenerate the MEA solution. Kinetic plots of solution pH and CO₂ loading for a series of 2.0 M MEA mineralization measurements are shown in Figure 7. For clarity, the mineralization measurements are separated here into four stages to determine the sensitivity of the CO₂-loaded MEA mineralization process to changes in the LKD concentration. Initially, in step one (Figure 7a), 15.0 g of LKD was dosed into a 500.0 mL aliquot of a 2.0 M MEA solution with a CO₂ loading of 0.5 mol CO₂/mol MEA. Extended duration CO₂ mineralization was continued for approximately 2000 min (\sim 33.3 h) with the initial and final CO₂ loading of the MEA solution monitored by FTIR. As shown in Figure 7a, upon the addition of LKD, the solution pH rapidly increases from 9.0 to 10.1. This change (in pH) results from the strong alkalinity of the LKD mineral. Over the remaining duration of step one, the pH of the solution remained nearly constant. Following the completion of CO₂ mineralization in step one, separation of solid and liquid in the slurry was performed. The CO₂ loading level of the collected MEA solution was determined to have decreased by approximately 16–20% (final CO₂ loading around 0.42 mol/mol). The reduction in the CO₂ loading is attributable to the conversion of carbonate ions from liquid to solid due to CO₂ mineralization (see reaction R8).

Additional mineralization was performed by the introduction of additional LKD (10.0 g) to the filtered MEA solution remaining after step one, as shown in Figure 7b. Correspondingly, the pH of the solution rapidly increased from 10.1 to 10.6. With further CO₂ mineralization taking place, the pH of the solution reduces slightly and slowly. Following CO₂ mineralization (2000 min duration, total 4000 min mineralization from steps one and two), the CO₂ loading of the solution was measured at \sim 0.33 mol/mol.

The above processes were repeated for the third and fourth mineralization steps (Figure 7c,d), where an additional 15.0

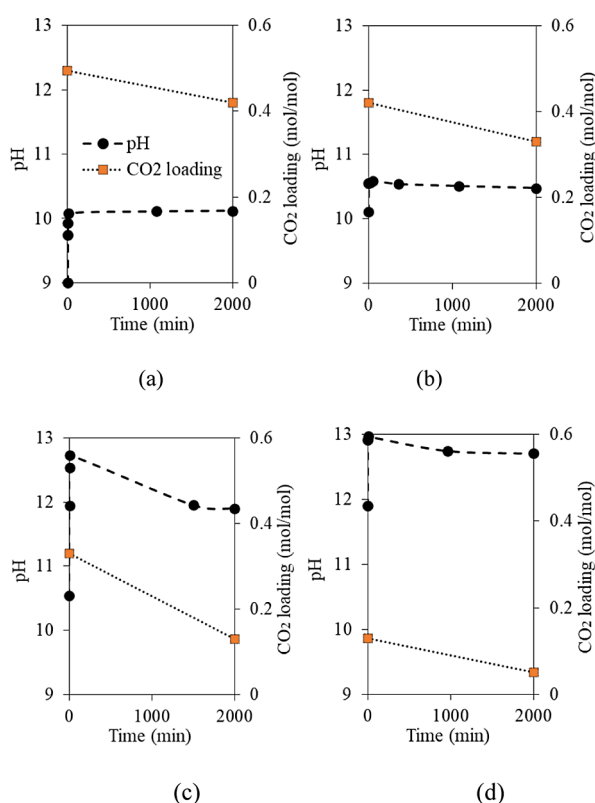


Figure 7. Multistep CO_2 desorption of CO_2 -loaded MEA solution by mineralization (a) first step, (b) second step, (c) third step, and (d) fourth step.

and 10.0 g of LKD was dosed into the collected MEA solutions at each step, respectively. Upon the addition of the LKD in the third step, the pH of the MEA solution rose dramatically from 10.4 to 12.7. Similarly, the addition of LKD in the fourth step produced a large initial step change in the pH of the solution (11.9–13.0). The final CO_2 loading in each of step three and four was similarly lower than the initial CO_2 loading and the previous steps (step 3 0.33–0.12 mol CO_2 /mol MEA, step 4 0.12–0.05 mol CO_2 /mol MEA), respectively. Importantly, the final CO_2 loading achieved here after four mineralization steps (0.05 mol of CO_2 /mol of MEA) indicates almost complete conversion of CO_2 in the MEA solutions have been achieved with some 90% of the absorption capacity regenerated for further CO_2 absorption cycling.

Mechanistic understanding of the mineralization processes is complex and dictated by both kinetic and equilibrium processes in the MEA solutions, leading to speciation changes as a function of the mineralization process. Initially, dosing of LKD in step one into the CO_2 -loaded MEA solution may be limiting the mineralization potential of the solution MEA,^{19,20,25} due to the limited formation of carbonate and bicarbonate ions. With continuous addition of LKD in subsequent dosing steps (two to four), alkaline hydrolysis of the carbamate may take place and promote further (and desirable) formation of the bicarbonate and carbonate ions driving the mineralization reaction with LKD. As carbonate is consumed by mineralization, the hydrolysis of carbamate to bicarbonate and carbonate (the ratio of which is strongly dependent on the pH of the solution) further drives the reaction equilibrium toward the formation of carbonate. From Figure 7a–d, with the continuous incorporation of LKD into

the CO_2 -loaded MEA solution, the added OH^- and Ca^{2+} finally lead to the precipitation of the sequestered CO_2 in the solution and thereby contribute to the regeneration of MEA. The potential for a direct mineralization reaction between carbamate and LKD is unclear but unlikely. To sum up, the low CO_2 mineralization reaction rate may be due mainly to (1) the slow conversion of carbamate to bicarbonate/carbonate, (2) the restrained leaching of calcium ions from LKD at alkaline conditions, and (3) the precipitation of calcium carbonates attached to the surface of LKD particles, which hinders further leaching of calcium from the LKD mineral.

3.2.2. Single-Step CO_2 Mineralization Method. Following from the multistep mineralization, a single-step CO_2 mineralization process with a specific liquid-to-solid ratio (25.0 g LKD dosed into 200.0 mL aliquot of 2.0 M MEA at 0.5 mol CO_2 /mol MEA) was performed. The initial pH of the CO_2 -loaded MEA solution was consistent with the initial solution in step one of the multistep measurements (i.e., pH 9). Following the addition of LKD, the pH of the solution increases ($\sim\text{pH } 12.7$) within 30 min of the LKD addition. As carbonation proceeds, the pH and CO_2 loading of the MEA solution decrease steadily as shown in Figure 8. Following

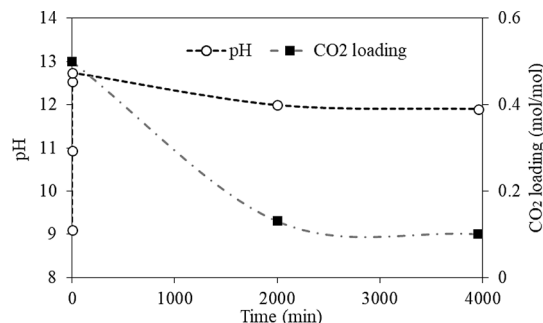


Figure 8. Single-step CO_2 mineralization of a 2.0 M MEA solution and 0.5 CO_2 loading (mole CO_2 /mol MEA) with LKD at ambient temperature.

mineralization for \sim 4000 min, the pH of the solution stabilizes ($\sim\text{pH } 11.9$) while the CO_2 loading has decreased to \sim 0.11 mol CO_2 /mol MEA. Similar to the multistep mineralization separation of solid and liquid was performed using a 0.45- μm membrane filter with the collected MEA solution (now CO_2 -lean) analyzed by FTIR and element ICP-OES for elemental concentrations as shown in Table 1. Correspondingly, the solid cake was subjected to SEM imaging (Figure 10), particle size analysis (Figure 11), and TGA analysis (Figure 12) after drying.

Table 1. Element Concentration in CO_2 -Lean 2.0 MEA Solution after Mineralization (ppm)

Ca	Si	Mg	Fe	Al
6	7	<1	<1	<1

FTIR analysis of the MEA solution is shown in Figure 9. The peak at 1360 cm^{-1} was assigned here to carbonate/bicarbonate, while carbamate, which has several FTIR active bands, was monitored by peaks at 1486 and 1568 cm^{-1} .^{25,28,29,31,33,34} After CO_2 mineralization, the FTIR spectra indicate that the MEA solution is CO_2 lean and almost free of carbamate/bicarbonate. This demonstrates the effectiveness of

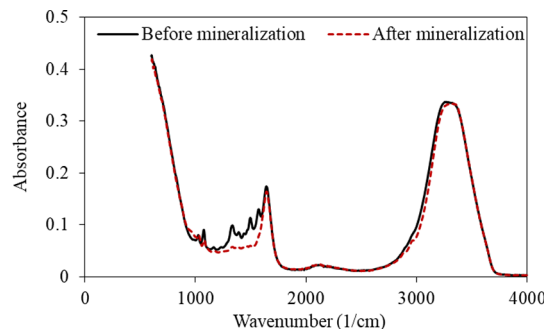
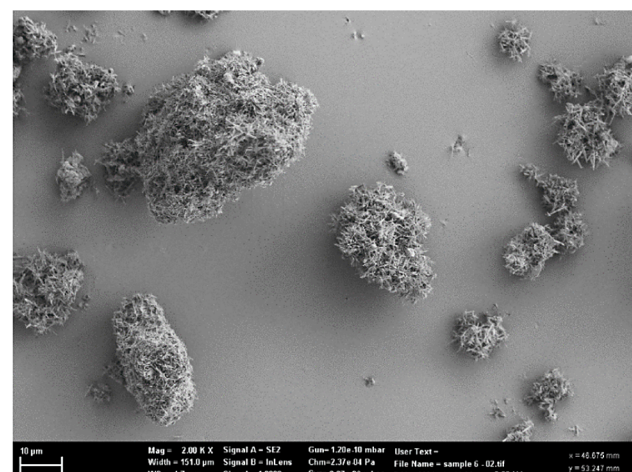


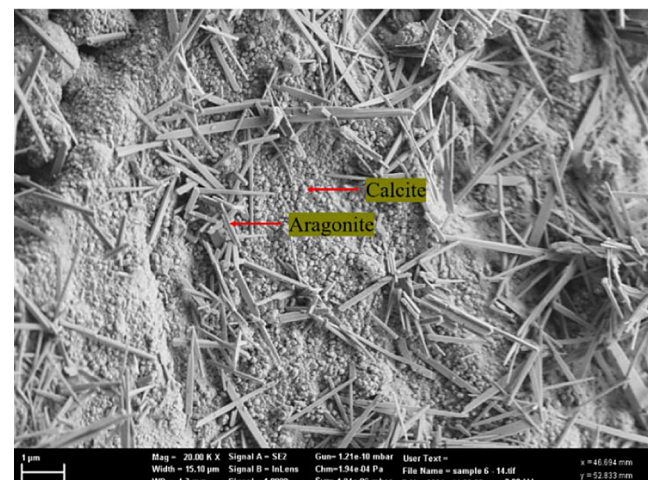
Figure 9. FTIR spectrum of 2.0 M MEA solution containing 0.5 mol CO_2/mol MEA pre- and post- CO_2 mineralization processing.

mineralization as a regeneration method. It can be noted from Table 1 that key elemental concentrations (of dissolved metals) are below 10 ppm. In particular, the low calcium concentration indicates that almost all calcium ions leached from LKD are precipitated during the carbonation process. Figure 10 shows SEM images following the carbonation of LKD (residue), indicating that calcite and aragonite are the primary calcium carbonate crystals formed during the mineralization of CO_2 in the MEA solutions. Interestingly, the particle size (of LKD, see Figure 11) reduces from (D50) 10.5 to 5.0 μm following mineralization. Naturally, the proportion of particles over 10 μm reduces, while the volume of smaller particles below 10 μm increases, indicating that the size of the precipitated calcium carbonates is generally below 10 μm . Besides, the decomposition of raw LKD particles after the leaching of calcium ions also contributes to the reduced particle size after the CO_2 mineralization. The TGA analysis of the mineralization product is shown in Figure 12. From the Figure, the capacity of the material was measured at ~ 230.0 g CO_2 per kg of LKD. Similarly, the theoretical mineralization capacity of LKD utilizing the change in CO_2 loading of the MEA solution as measured by FTIR was estimated at ~ 256 g CO_2 per kg.

3.3. Temperature Effect on CO_2 Mineralization. From the data in Section 3.2, the ability of CO_2 mineralization to decarbonize a CO_2 -loaded MEA solution is kinetically limited at ambient temperature conditions. To further explore and optimize the mineralization process conditions for rapid MEA regeneration, the effect of temperature on the CO_2 mineralization process was investigated here. A series of 2.0 M MEA solutions with various CO_2 loadings from 0.26 to 0.55 mol CO_2/mol MEA were evaluated here for their mineralization potential with LKD at a range of temperatures from 40.0 to 60.0 $^\circ\text{C}$, respectively. In this series, 200 mL solutions were individually dosed with ~ 15 g of LKD with the corresponding reaction curves shown in Figure 13. From the data, an increase in reaction temperature has a positive and dramatic effect on the mineralization rate in the MEA solutions which improves the corresponding mineralization time from some 2000 min at ambient temperature to some 250–400 min at elevated temperatures. Additionally, the elevated temperature promotes deeper MEA regeneration to lower CO_2 loadings (~ 0.06 mol/mol, CO_2 desorption efficiency up to ~ 79 to 83%). Notably, the most significant improvement in the mineralization process is observed from the initial increase in the solution temperature from ambient to 40 $^\circ\text{C}$, with further improvements (up to 60 $^\circ\text{C}$) yielding only slight improvements. The mild increase from ambient temperature to 40 $^\circ\text{C}$ is well within the boundaries of



(a)

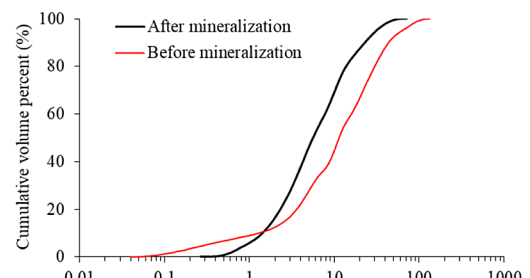


(b)

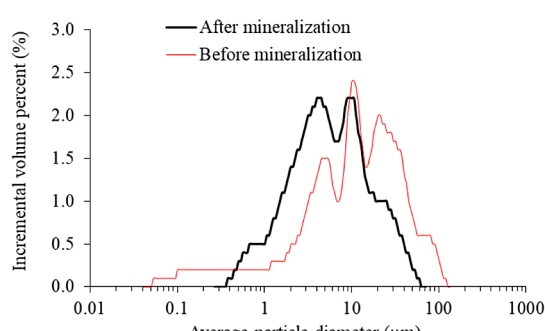
Figure 10. SEM images of LKD post mineralization at various scales (a) 10.0 and (b) 1.0 μm .

waste heat integration from other industrial processes or solar-driven heating methods. It should be noted that the above improvement in the mineralization efficiency with increasing temperature is correspondingly influenced by the initial CO_2 loading of the solutions and the concentration of LKD dosed into the solutions, with longer mineralization times required for elevated CO_2 loadings. This is demonstrated in Figure 13d, where the mineralization process begins to stabilize as the CO_2 loading approaches 0.3 mol/mol at 60 $^\circ\text{C}$ due to exhaustion of the LKD. This is further demonstrated in the TGA analysis of the samples in Figure 14, where the determined CO_2 capacity is approximately 236 g CO_2 per kg LKD. Precipitated calcium carbonates at elevated temperatures are similar to those formed under ambient mineralization conditions (i.e., aragonite and calcite), as shown in Figure 15. However, a comparison of the crystals formed at elevated temperatures indicates they are seemingly coarser.

The main mechanisms leading to the fast CO_2 mineralization at elevated temperatures (between 40 and 60 $^\circ\text{C}$) may be



(a)



(b)

Figure 11. Particle size of LKD pre- and post-CO₂ mineralization (a) cumulative volume percent and (b) incremental volume percent.

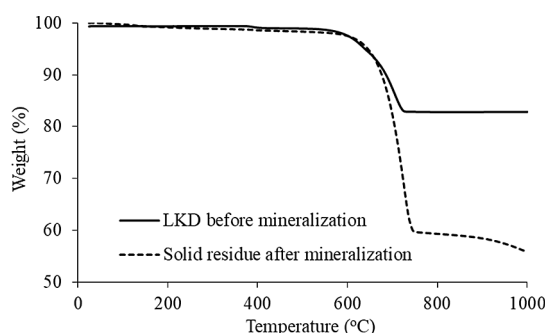
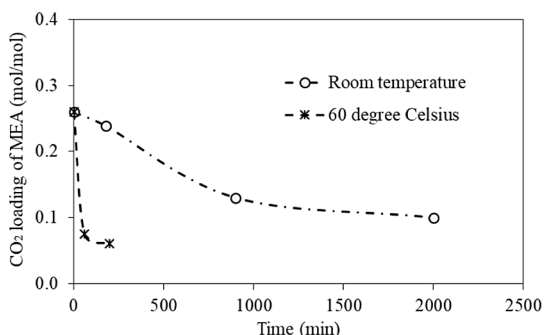
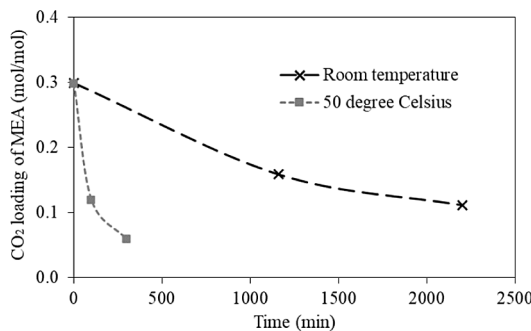


Figure 12. TGA analysis of solid LKD residue after CO₂ mineralization in a 2.0 M MEA solution with 0.5 CO₂ loading (mol of CO₂/mol of MEA).

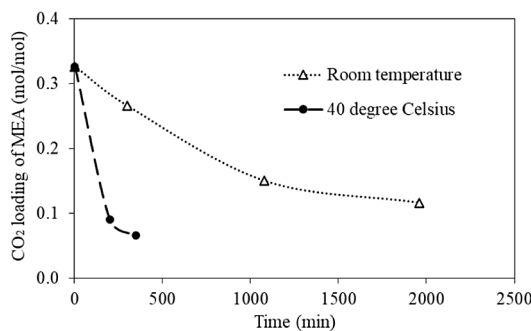
attributed to the fact that both kinetics of carbonation reactions and leaching of calcium from LKD are accelerated by temperature rise (as indicated by the Arrhenius equation).^{22,25,27,35–38} Following the above acceleration effect, the conversion of carbamate to bicarbonate is therefore promoted upon CO₂ mineralization at an increased temperature.³⁹ Last but not least, it should be clarified that the reaction between CO₂ and MEA is exothermic and the flue gas emitted by industries generally has a relatively high temperature. The reaction heat and latent heat present in flue gas may be utilized to raise the temperature of the CO₂-loaded MEA solution for mineralization, potentially enhancing energy efficiency.^{19,25} Besides, to facilitate CO₂ absorption, pretreatment of flue gases is required to remove solid particulates and other impurities.^{40,41} A pretreatment system may contribute to overall capital cost, especially if desulfurization of flue gas is needed.



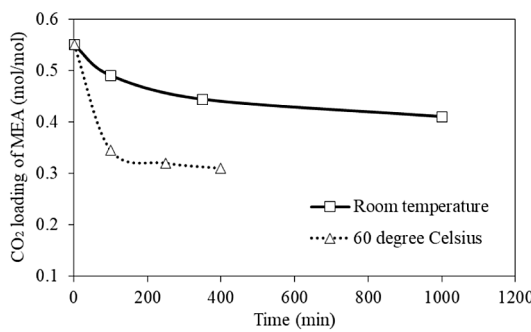
(a)



(b)



(c)



(d)

Figure 13. Effect of temperature on CO₂ desorption of MEA with different initial CO₂ loadings (a) 0.26 mol/mol, (b) 0.30 mol/mol, (c) 0.32 mol/mol, and (d) 0.55 mol/mol.

4. RESEARCH GAP AND FUTURE PROSPECTS

4.1. Other Amines. In addition to MEA, many different amines have been investigated for postcombustion carbon capture,^{5,10,12,17,23,25,29} such as 2-amino-2-methyl-1propanol

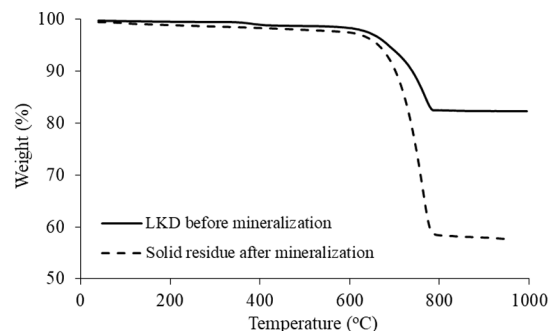


Figure 14. TGA analysis of solid residue of LKD after CO_2 mineralization with 2.0 M MEA at 0.55 CO_2 loading (mol of CO_2 /mol of MEA) at 60.0 °C.

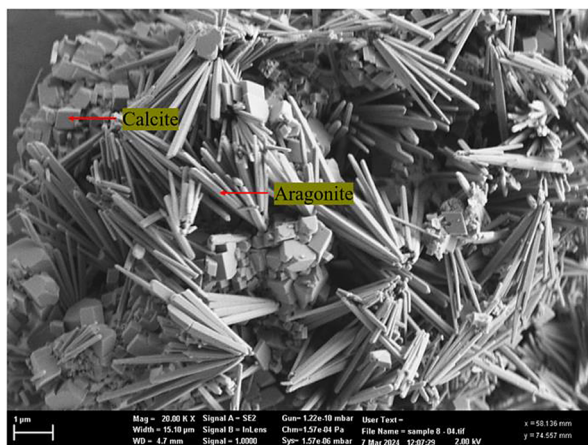


Figure 15. SEM image of LKD after CO_2 mineralization with 2.0 M MEA at 0.55 CO_2 loading (mol of CO_2 /mol of MEA) at 60.0 °C.

(AMP), diethanolamine (DEA), methyldiethanolamine (MDEA), piperazine (PZ), and triethanolamine (TEA). Generally, a high content of bicarbonate/carbonate ions in amine solutions after CO_2 capture appears to be desirable for the purpose of CO_2 mineralization. Based on such a criterion, DEA, MDEA, and AMP may be applicable for the integrated CO_2 capture and mineralization approach,^{25,29} but further verification is needed by experiments. According to the discussions given in Section 3.2, the presence of both hydroxide and calcium ions is of critical importance for the conversion of carbamate to bicarbonate/carbonate. Such conversions of different amines under different conditions (e.g., temperature, pressure, and concentration) should be explored in-depth in the future.

4.2. Washing and Reuse of Solid. Washing and reuse of LKD solid residue after CO_2 mineralization is of considerable importance for the deployment of the amine-based CO_2 capture and mineralization approach at a commercial scale. This can (1) minimize mass loss of amines, thereby promoting the recycling and reuse of amines and reducing the operating costs of the integrated CO_2 capture and mineralization technologies, and (2) promote the utilization of the carbonated LKD solid as valuable byproducts. For CO_2 mineralization, due to the high water absorption capacity of the precipitated calcium carbonates, minimization of loss of the absorption liquid is a challenge. To reduce the cost induced by the mass loss, recollection of the MEA residue absorbed by the LKD solid after CO_2 mineralization may be carried out by

washing. However, the amine washed from the carbonated solid residue is correspondingly difficult to concentrate.²³ To overcome this challenge requires further research. After washing, due to the high content of calcium carbonates, the carbonated LKD solid may be used for additional purposes, such as construction materials, painting and coating materials, and papermaking materials among other uses.⁴² In particular, if the precipitated calcium carbonates are of sufficiently high purity, then the value of the (carbonate) product may significantly offset the operating costs of the integrated CO_2 capture and mineralization process.

4.3. Other CO_2 Mineralization Feedstocks. In the proposed integrated CO_2 capture and mineralization process, large quantities of CO_2 mineralization feedstock are required to process the absorption liquid, particularly at industrial scales, for the impact on CO_2 emissions reduction. A single alkaline solid waste material (e.g., LKD used in this study) is unlikely to provide the capacity required to meet the rising demand for CO_2 mineral sequestration. In previous studies,^{22,37,43–45} a wide range of alkaline materials have been recommended as CO_2 mineralization feedstocks. According to the current study, for CO_2 mineralization in amine solutions, besides calcium ions, hydroxide ions provided by and present in CO_2 mineral feedstocks also tend to play an important role. Compared to alkaline minerals mainly containing calcium or magnesium silicates, alkaline solids with high CaO/MgO and/or $\text{Ca}(\text{OH})_2/\text{Mg}(\text{OH})_2$ content seem more favorable for deployment in the integrated CO_2 capture and mineralization process with aqueous amines as the CO_2 capture agent. Furthermore, for alkaline solid wastes with a high content of calcium/magnesium silicates (i.e., wollastonite, ultramafic tailings, and other mafic rocks), an additional activation process may be required to increase their CO_2 mineralization reactivity and thereby increase the regeneration efficiency of amines by CO_2 mineralization. The mineralization behaviors of different calcium and magnesium minerals within aqueous amine solutions may vary significantly, requiring further research efforts.

5. CONCLUSIONS

As part of global CCUS strategies and technologies, the integrated CO_2 capture and mineralization technology can take advantage of postcombustion carbon capture with permanent CO_2 sequestration to support hard-to-abate industries to reach net zero emissions. In this study, the integrated CO_2 capture and mineralization approach based on MEA was explored in-depth, focusing on the deployment of CO_2 mineralization with LKD to decarbonize CO_2 -loaded aqueous MEA solutions. Using LKD to recover or decarbonize an MEA solution subjected to CO_2 capture is feasible, while the recovery process based on CO_2 mineralization at room temperature tends to be kinetically limited. Both solution pH and temperature are two critical levers influencing the CO_2 mineralization kinetics. When the pH of MEA solvent is higher than ~10.5, CO_2 mineralization takes place considerably faster than that at a lower pH level where CO_2 mineralization is quite limited. Increasing the mineralization temperature has a positive and dramatic effect on the mineralization rate in the MEA solutions, which was found to improve the corresponding mineralization time by some 4–5 times that of the ambient measurements. Correspondingly, the elevated temperature also promotes deeper MEA regeneration to a much lower CO_2 loading (~0.06 mol CO_2 /mol MEA). The mechanisms behind

the influences of pH and temperature on the accelerated CO₂ desorption of the MEA solvent are elaborated. Besides, after CO₂ mineralization of LKD in MEA solvent, calcite and aragonite are observed as primary calcium carbonates precipitated, and the measured CO₂ sequestration capacity of LKD is around 230 g of CO₂ per kg. For the upgraded development of the integrated CO₂ capture and mineralization technology, key research gaps are identified and discussed in this paper, and further research is also underlined.

AUTHOR INFORMATION

Corresponding Authors

Liang Li – CSIRO Energy, Newcastle, NSW 2304, Australia;
✉ orcid.org/0000-0001-7502-8751; Email: liang.li@csiro.au

Hai Yu – CSIRO Energy, Newcastle, NSW 2304, Australia;
✉ orcid.org/0000-0002-4552-9552; Email: Hai.yu@csiro.au

Authors

Graeme Puxty – CSIRO Energy, Newcastle, NSW 2304, Australia; ✉ orcid.org/0000-0002-6880-7594

Song Zhou – CSIRO Energy, Newcastle, NSW 2304, Australia

William Conway – CSIRO Energy, Newcastle, NSW 2304, Australia; ✉ orcid.org/0000-0002-7958-3872

Paul Feron – CSIRO Energy, Clayton, VIC 3168, Australia

Complete contact information is available at:

<https://pubs.acs.org/10.1021/acs.iecr.4c02064>

Notes

The authors declare no competing financial interest.

ACKNOWLEDGMENTS

The first author thanks the financial support provided through the CSIRO Early Research Career Fellowship program. Part of this work also received financial support from the HILT CRC (Heavy Industry Low-carbon Transition Cooperative Research Centre, Australia), which is sincerely acknowledged.

REFERENCES

- (1) Geerlings, H.; Zevenhoven, R. CO₂ mineralization—Bridge Between Storage and Utilization of CO₂. *Annu. Rev. Chem. Biomol. Eng.* **2013**, *4* (1), 103–117.
- (2) International Energy Agency. *Energy Technology Perspectives 2020 - Special Report on Carbon Capture Utilisation and Storage: CCUS in clean energy transitions*; OECD Publishing: Paris, 2020.
- (3) Verein Deutscher Zementwerke e.V. *Decarbonisation Pathways for the Australian Cement Sector*; VDZ: Germany, 2021.
- (4) Dutcher, B.; Fan, M.; Russell, A. G. Amine-Based CO₂ Capture Technology Development from the Beginning of 2013—A Review. *ACS Appl. Mater. Interfaces* **2015**, *7* (4), 2137–2148.
- (5) Liang, Z. H.; Rongwong, W.; Liu, H.; Fu, K.; Gao, H.; Cao, F.; Zhang, R.; Sema, T.; Henni, A.; Sumon, K.; Nath, D.; Gelowitz, D.; Srisang, W.; Saiwan, C.; Benamor, A.; Al-Marri, M.; Shi, H.; Supap, T.; Chan, C.; Zhou, Q.; Abu-Zahra, M.; Wilson, M.; Olson, W.; Idem, R.; Tontiwachwuthikul, P. (Pt). Recent Progress and New Developments in Post-Combustion Carbon-Capture Technology with Amine Based Solvents. *Int. J. Greenhouse Gas Control* **2015**, *40*, 26–54.
- (6) Khalilpour, R.; Mumford, K.; Zhai, H.; Abbas, A.; Stevens, G.; Rubin, E. S. Membrane-Based Carbon Capture from Flue Gas: A Review. *Journal of Cleaner Production* **2015**, *103*, 286–300.
- (7) Feron, P. H. M.; Cousins, A.; Jiang, K.; Zhai, R.; Garcia, M. An Update of the Benchmark Post-Combustion CO₂-Capture Technology. *Fuel* **2020**, *273*, No. 117776.
- (8) Chao, C.; Deng, Y.; Dewil, R.; Baeyens, J.; Fan, X. Post-Combustion Carbon Capture. *Renewable and Sustainable Energy Reviews* **2021**, *138*, No. 110490.
- (9) Global CCS Institute. *Global Status of CCS 2022*; Global CCS Institute, 2022.
- (10) Puxty, G.; Rowland, R.; Allport, A.; Yang, Q.; Bown, M.; Burns, R.; Maeder, M.; Attalla, M. Carbon Dioxide Postcombustion Capture: A Novel Screening Study of the Carbon Dioxide Absorption Performance of 76 Amines. *Environ. Sci. Technol.* **2009**, *43* (16), 6427–6433.
- (11) Strazisar, B. R.; Anderson, R. R.; White, C. M. Degradation Pathways for Monoethanolamine in a CO₂ Capture Facility. *Energy Fuels* **2003**, *17* (4), 1034–1039.
- (12) Simon, L. L.; Elias, Y.; Puxty, G.; Artanto, Y.; Hungerbuhler, K. Rate Based Modeling and Validation of a Carbon-Dioxide Pilot Plant Absorption Column Operating on Monoethanolamine. *Chem. Eng. Res. Des.* **2011**, *89* (9), 1684–1692.
- (13) Zhang, Z.; Li, Y.; Zhang, W.; Wang, J.; Soltanian, M. R.; Olabi, A. G. Effectiveness of Amino Acid Salt Solutions in Capturing CO₂: A Review. *Renewable and Sustainable Energy Reviews* **2018**, *98*, 179–188.
- (14) Vega, F.; Sanna, A.; Navarrete, B.; Maroto-Valer, M. M.; Cortés, V. J. Degradation of Amine-Based Solvents in CO₂ Capture Process by Chemical Absorption. *Greenhouse Gas Sci. Technol.* **2014**, *4* (6), 707–733.
- (15) Feron, P. H. M. The Potential for Improvement of the Energy Performance of Pulverized Coal Fired Power Stations with Post-Combustion Capture of Carbon Dioxide. *Energy Procedia* **2009**, *1* (1), 1067–1074.
- (16) Anderson, S.; Newell, R. Prospects for Carbon Capture and Storage Technologies. *Annu. Rev. Environ. Resour.* **2004**, *29* (1), 109–142.
- (17) Samarakoon, P. A. G. L.; Andersen, N. H.; Perinu, C.; Jens, K.-J. Equilibria of MEA, DEA and AMP with Bicarbonate and Carbamate: A Raman Study. *Energy Procedia* **2013**, *37*, 2002–2010.
- (18) McCann, N.; Phan, D.; Wang, X.; Conway, W.; Burns, R.; Attalla, M.; Puxty, G.; Maeder, M. Kinetics and Mechanism of Carbamate Formation from CO₂ (Aq), Carbonate Species, and Monoethanolamine in Aqueous Solution. *J. Phys. Chem. A* **2009**, *113* (17), 5022–5029.
- (19) Lv, B.; Guo, B.; Zhou, Z.; Jing, G. Mechanisms of CO₂ Capture into Monoethanolamine Solution with Different CO₂ Loading during the Absorption/Desorption Processes. *Environ. Sci. Technol.* **2015**, *49* (17), 10728–10735.
- (20) Conway, W.; Wang, X.; Fernandes, D.; Burns, R.; Lawrence, G.; Puxty, G.; Maeder, M. Comprehensive Kinetic and Thermodynamic Study of the Reactions of CO₂ (Aq) and HCO₃⁻ with Monoethanolamine (MEA) in Aqueous Solution. *J. Phys. Chem. A* **2011**, *115* (50), 14340–14349.
- (21) Liu, M.; Gadikota, G. Integrated CO₂ Capture, Conversion, and Storage To Produce Calcium Carbonate Using an Amine Looping Strategy. *Energy Fuels* **2019**, *33* (3), 1722–1733.
- (22) Yan, Z.; Wang, Y.; Yue, H.; Liu, C.; Zhong, S.; Ma, K.; Liao, W.; Tang, S.; Liang, B. Integrated Process of Monoethanolamine-Based CO₂ Absorption and CO₂ mineralization with SFGD Slag: Process Simulation and Life-Cycle Assessment of CO₂ Emission. *ACS Sustainable Chem. Eng.* **2021**, *9* (24), 8238–8248.
- (23) Ji, L.; Zhang, L.; Zheng, X.; Feng, L.; He, Q.; Wei, Y.; Yan, S. Simultaneous CO₂ Absorption, Mineralisation and Carbonate Crystallisation Promoted by Amines in a Single Process. *Journal of CO₂ Utilization* **2021**, *51*, No. 101653.
- (24) Hong, S.; Sim, G.; Moon, S.; Park, Y. Low-Temperature Regeneration of Amines Integrated with Production of Structure-Controlled Calcium Carbonates for Combined CO₂ Capture and Utilization. *Energy Fuels* **2020**, *34* (3), 3532–3539.
- (25) Zhang, W.; Xu, Y.; Wang, Q. Coupled CO₂ Absorption and Mineralization with Low-Concentration Monoethanolamine. *Energy* **2022**, *241*, No. 122524.
- (26) Li, L.; Yu, H.; Ji, L.; Zhou, S.; Dao, V.; Feron, P.; Benhelal, E. Integrated CO₂ Capture and Mineralization Approach Based on

KOH and Cement-Based Wastes. *Journal of Environmental Chemical Engineering* **2024**, *12* (5), No. 113382.

(27) Li, L.; Liu, Q.; Dao, V.; Wu, M. Dimensional Change of Cement Paste Subjected to Carbonation in CO₂ Sequestration and Utilization Context: A Critical Review on the Mechanisms. *Journal of CO₂ Utilization* **2023**, *70*, No. 102444.

(28) Sun, C.; Dutta, P. K. Infrared Spectroscopic Study of Reaction of Carbon Dioxide with Aqueous Monoethanolamine Solutions. *Ind. Eng. Chem. Res.* **2016**, *55* (22), 6276–6283.

(29) Richner, G.; Puxty, G. Assessing the Chemical Speciation during CO₂ Absorption by Aqueous Amines Using in Situ FTIR. *Ind. Eng. Chem. Res.* **2012**, *51* (44), 14317–14324.

(30) Puxty, G.; Bennett, R.; Conway, W.; Webster-Gardiner, M.; Yang, Q.; Pearson, P.; Cottrell, A.; Huang, S.; Feron, P.; Reynolds, A.; Verheyen, V. IR Monitoring of Absorbent Composition and Degradation during Pilot Plant Operation. *Ind. Eng. Chem. Res.* **2020**, *59* (15), 7080–7086.

(31) Jackson, P.; Robinson, K.; Puxty, G.; Attalla, M. In Situ Fourier Transform-Infrared (FT-IR) Analysis of Carbon Dioxide Absorption and Desorption in Amine Solutions. *Energy Procedia* **2009**, *1* (1), 985–994.

(32) Puxty, G.; Maeder, M. A Simple Chemical Model to Represent CO₂-Amine-H₂O Vapour-Liquid-Equilibria. *International Journal of Greenhouse Gas Control* **2013**, *17*, 215–224.

(33) Du Preez, L. J.; Motang, N.; Callanan, L. H.; Burger, A. J. Determining the Liquid Phase Equilibrium Speciation of the CO₂ – MEA–H₂O System Using a Simplified in Situ Fourier Transform Infrared Method. *Ind. Eng. Chem. Res.* **2019**, *58* (1), 469–478.

(34) Shohrat, A.; Zhang, M.; Hu, H.; Yang, X.; Liu, L.; Huang, H. Mechanism Study on CO₂ Capture by Ionic Liquids Made from TFA Blended with MEA and MDEA. *International Journal of Greenhouse Gas Control* **2022**, *119*, No. 103709.

(35) Coto, B.; Martos, C.; Peña, J. L.; Rodríguez, R.; Pastor, G. Effects in the Solubility of CaCO₃: Experimental Study and Model Description. *Fluid Phase Equilib.* **2012**, *324*, 1–7.

(36) De Larrard, T.; Benboudjema, F.; Colliat, J. B.; Torrenti, J. M.; Deleruyelle, F. Concrete Calcium Leaching at Variable Temperature: Experimental Data and Numerical Model Inverse Identification. *Comput. Mater. Sci.* **2010**, *49* (1), 35–45.

(37) Li, L.; Yu, H.; Zhou, S.; Dao, V.; Chen, M.; Ji, L.; Benhelal, E. Activation and Utilization of Tailings as CO₂ mineralization Feedstock and Supplementary Cementitious Materials: A Critical Review. *Materials Today Sustainability* **2023**, *24*, No. 100530.

(38) Wang, F.; Dreisinger, D.; Jarvis, M.; Hitchins, T. Kinetics and Mechanism of Mineral Carbonation of Olivine for CO₂ Sequestration. *Minerals Engineering* **2019**, *131*, 185–197.

(39) Wada, S.; Kushida, T.; Itagaki, H.; Shibue, T.; Kadowaki, H.; Arakawa, J.; Furukawa, Y. ¹³C NMR Study on Carbamate Hydrolysis Reactions in Aqueous Amine/CO₂ Solutions. *International Journal of Greenhouse Gas Control* **2021**, *104*, No. 103175.

(40) Srivastava, R. K.; Jozewicz, W. Flue Gas Desulfurization: The State of the Art. *J. Air Waste Manage. Assoc.* **2001**, *51* (12), 1676–1688.

(41) Sayari, A.; Belmabkhout, Y.; Serna-Guerrero, R. Flue Gas Treatment via CO₂ Adsorption. *Chemical Engineering Journal* **2011**, *171* (3), 760–774.

(42) Jimoh, O. A.; Ariffin, K. S.; Hussin, H. B.; Temitope, A. E. Synthesis of Precipitated Calcium Carbonate: A Review. *Carbonates Evaporites* **2018**, *33* (2), 331–346.

(43) Gadikota, G.; Matter, J.; Kelemen, P.; Brady, P. V.; Park, A.-H. A. Elucidating the Differences in the Carbon Mineralization Behaviors of Calcium and Magnesium Bearing Alumino-Silicates and Magnesium Silicates for CO₂ Storage. *Fuel* **2020**, *277*, No. 117900.

(44) Li, L.; Wu, M. An Overview of Utilizing CO₂ for Accelerated Carbonation Treatment in the Concrete Industry. *Journal of CO₂ Utilization* **2022**, *60*, No. 102000.

(45) Gadikota, G.; Park, A. A. Accelerated Carbonation of Ca- and Mg-Bearing Minerals and Industrial Wastes Using CO₂. In *Carbon Dioxide Utilisation*; Elsevier, 2015; pp. 115–137.